ECS Transactions, 11 (1) 241-247 (2007)
10.1149/1.2780936 ©The Electrochemical Society

Highly Active Carbon Composite Electrocatalysts for PEM Fuel Cells

Vijayadurga Nallathambi, Gang Wu, Nalini P. Subramanian, Swaminatha P. Kumaraguru, Jong-Won Lee, and Branko N. Popov

Department of Chemical Engineering, University of South Carolina, Columbia, South Carolina 29208, USA

Highly active carbon composite catalysts were developed using a carbon based metal-free catalyst developed at USC as a support through catalyzed pyrolysis followed by chemical post-treatments. Materials characterization studies indicated that the nature of nitrogen functional groups on the carbon surface and the carbon nanostructures play a critical role in the activity and stability. The catalytic activity as high as 2.0 A cm^{-2} at 0.2 V was obtained for the carbon composite catalyst in the fuel cell, and no irreversible activity loss was observed during stability test.

Introduction

Since Jasinski's discovery of the catalytic properties of Co phthalocyanines for oxygen reduction (1), there has been a considerable research on non-precious metal catalysts such as: (i) porphyrin-based macrocyclic compounds of transition metal (2-18), (ii) vacuum-deposited cobalt and iron compounds (e.g. Co-C-N and Fe-C-N) (19, 20) and (iii) metal carbides, nitrides and oxides (e.g. FeC_x, TaO_xN_y, MnO_x/C) (21, 22). Pyrolysis at higher temperatures than 800 ^oC in an inert or NH_3 atmosphere led to the improvement in catalytic activity of the catalysts to some extent.

Recently, we synthesized a Co-based catalyst using low-cost precursors and surface-modifiers, and loaded on carbon activated with a procedure developed at USC (23-25). The observed onset potential for oxygen reduction was as high as 0.85 V vs. SHE, which was higher than any other reported in the literature. However, due to low selectivity (H_2O_2 amount > 5%) and poor stability observed in case of Co, Fe, Fe-Co, Ni, and Se, the transition metal-based catalysts reported in the literature so far do not qualify as catalyst for oxygen reduction.

The objective of this work is to develop highly active and stable carbon-based metal-free catalysts and carbon composite catalysts with strong Lewis basicity (π electron delocalization) to facilitate the oxygen reduction reaction. The active reaction sites for oxygen reduction were optimized as a function of: (ii) surface oxygen groups, (ii) nitrogen content, (iii) pyrolysis temperature, (iv) the concentration of the non-metallic additives, and (v) metal concentration.

Experimental

Catalyst Synthesis

Carbon-based metal-free catalysts were synthesized by modifying the surface functional groups on the porous carbon black with nitrogen-containing organic precursors.

As a next step, carbon composite catalysts were developed using a metal-free catalyst as a support through "catalyzed pyrolysis", followed by chemical post-treatments.

Rotating Ring-Disk Electrode (RRDE) Experiments

The RRDE measurements were performed in a three-electrode electrochemical cell using a bi-potentiostat (Pine Instruments) at room temperature. An RRDE with gold ring (5.52 mm inner-diameter and 7.16 mm outer-diameter) and glassy carbon disk (5.0 mm diameter) was employed as the working electrode. The catalyst ink was prepared by blending the catalyst powder with isopropyl alcohol in an ultrasonic bath. The catalyst ink was deposited onto the glassy carbon disk which was previously polished with Al_2O_3 powder. After drying, a mixture of Nafion™ solution (5 wt%, Aldrich) and isopropyl alcohol was coated onto the catalyst layer to ensure better adhesion of the catalyst on the glassy carbon substrate. The electrolyte was 0.5 M H_2SO_4 solution. A platinum mesh and $Hg/HgSO_4$ electrode were used as the counter and reference electrodes, respectively. All potentials in this work were referred to a standard hydrogen electrode (SHE).

In order to estimate the double layer capacitance, the electrolyte was deaerated by bubbling with N_2, and the cyclic voltammogram was recorded by scanning the disk potential between 0.04 and 1.04 V(SHE) at rate of 5 mV s^{-1}. Then, the electrocatalytic activity for oxygen reduction was evaluated in the oxygen-saturated electrolyte. The oxygen reduction current was taken as the difference between currents measured in the deaerated and oxygen-saturated electrolytes. The ring potential was held at 1.2 V(SHE) to oxidize H_2O_2 generated during the oxygen reduction reaction.

Performance Test of Membrane-Electrode Assemblies (MEAs)

The cathode catalyst ink was prepared by ultrasonically blending catalyst with Nafion™ solution and isopropyl alcohol for 4 h. The catalyst ink was then sprayed onto a gas diffusion layer (GDL) (ELAT LT 1400W, E-TEK) until a desired catalyst loading has been achieved. A commercially catalyzed GDL (0.5 mg_{Pt} cm^{-2}, E-TEK) was used as the anode. A thin layer of Nafion™ was coated on both the cathode and anode surfaces. The Nafion™-coated anode and cathode were hot-pressed to a Nafion™ 112 membrane at 140 ^oC and 534 kPa for 3 min. The geometric area of the electrode was 5 cm^2.

The MEA tests were carried out in a single cell with serpentine flow channels. Pure H_2 gas humidified at 77 ^oC and pure O_2 gas humidified at 75 ^oC were supplied to the anode and cathode compartments, respectively. The measurements were conducted using a fully automated test station (Fuel Cell Technologies Inc.) at 75 ^oC. In order to evaluate the stability of catalyst, potentiostatic current transient technique was used by applying a constant potential of 0.4 or 0.5 V.

Results and Discussion

Figure 1(a) presents the fuel cell performances loaded with 6 mg cm^{-2} of the metal-free CN and C-X catalysts. Here, C, N and X stand for carbon, nitrogen and non-metallic additive, respectively. The tests were run with H_2 and O_2 using the back pressures of 30 and 40 psi, respectively. For the C-X catalyst, the current density was measured to be 1.3 A cm^{-2} at 0.2 V. Fig. 1(b) shows the current transient measured at 0.4 V for stability test

on the fuel cell loaded with 4 mg cm^{-2} of the C-N catalyst. The result shows an initial increase of current density to ca. 0.12 A cm^{-2} and then a steady-state current profile without showing performance degradation for up to 200 h.

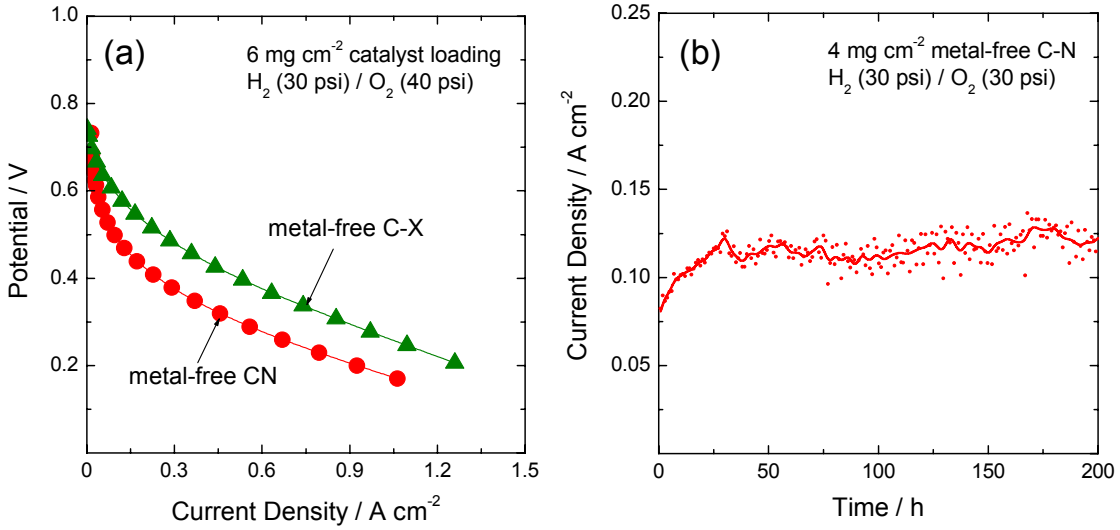

Figure 1. (a) Fuel cell performances of the metal-free CN and C-X catalysts, and (b) stability test data (at 0.4 V) for the CN catalyst.

Figure 2(a) and (b) present polarization curves on the rotating disk electrodes and the percentages of H_2O_2 produced during oxygen reduction, respectively, for the carbon composite catalysts supported on (i) the oxidized carbon and (ii) the metal-free catalyst. The carbon composite catalyst supported on the metal-free catalyst shows higher activity and selectivity (less than 1% H_2O_2 at 0.5 V vs. SHE) as compared with the catalyst on the oxidized carbon (6% H_2O_2), which is due to higher catalytic selectivity of metal-free catalyst support (less than 1% H_2O_2) (data not shown).

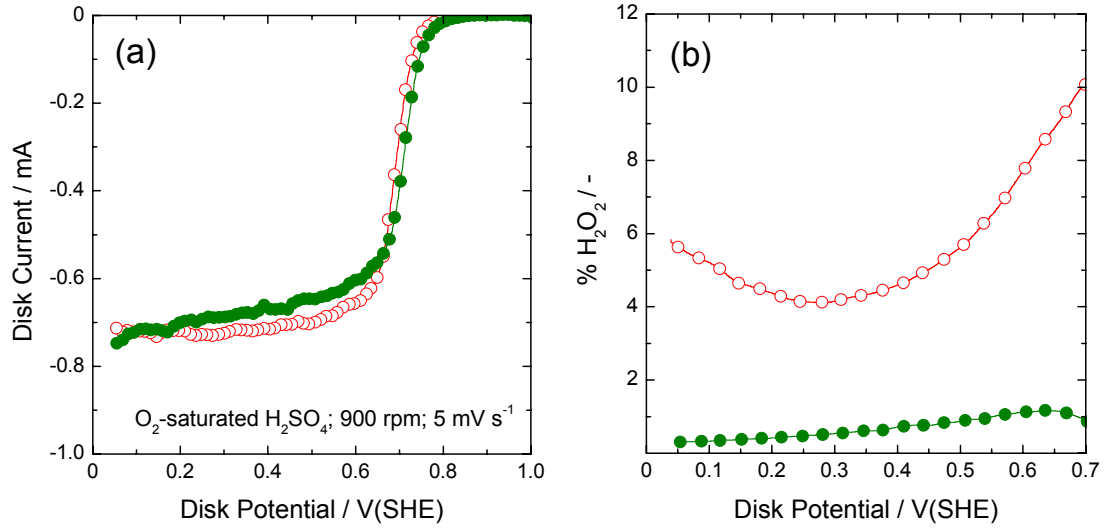

Figure 2. (a) Catalytic activity and (b) selectivity in RRDE for the carbon composite catalysts supported on the oxidized carbon (open circle) and the metal-free catalyst (closed circle).

The nature of nitrogen functional groups were identified using X-ray photoelectron spectroscopy (XPS) at each synthesis step of the carbon composite catalyst: (i) before "catalyzed pyrolysis", (ii) after "catalyzed pyrolysis", and (iii) after chemical post-treatment, and the results are summarized in Table 1 along with the activity and selectivity data. The current density and % H_2O_2 were determined at 0.4 V in a fuel cell and an RRDE, respectively.

The activity and selectivity gradually increased after pyrolysis and after chemical post-treatment. XPS data obtained before pyrolysis show only nitrogen functional group in the N-precursor. High-temperature pyrolysis results in the formation of pyridinic, pyrrolic and graphitic nitrogen groups. Chemical post-treatment increases the relative concentration of pyridinic nitrogen, while removing pyrrolic nitrogen. XPS result indicates that high-temperature pyrolysis combined with chemical post-treatment increases the concentration of pyridine–type nitrogen resulting in the increased Lewis basicity, and incorporates the nitrogen into graphitic structures that increases the stability.

Table 1. Catalytic activity, selectivity and XPS spectrum at each synthesis step of carbon composite catalyst. The current density and % H_2O_2 were determined at 0.4 V in a fuel cell and an RRDE, respectively.

Step	Current Density (A cm^{-2})	% H_2O_2	XPS
Before pyrolysis	0	-	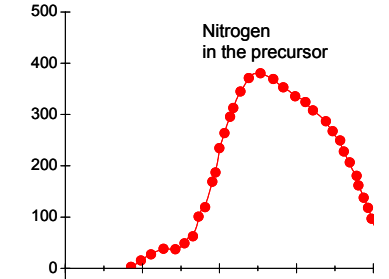
After pyrolysis	0.32	5	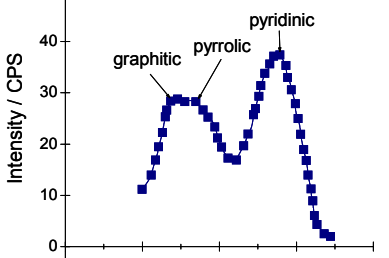
After chemical post-treatment	0.88	0.5	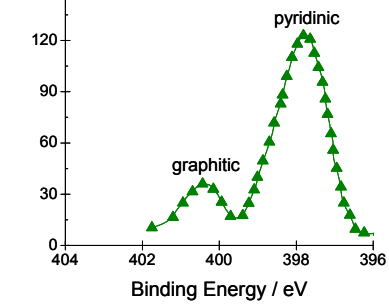

The catalyzed pyrolysis process was optimized to increase the concentration of active reaction sites and the stability. Figure 3(a) illustrates the fuel cell performances of carbon composite catalysts prepared under different pyrolysis conditions. The cathode catalyst loading was 4 mg cm^{-2}, and the tests were run with H_2 (30 psi) and O_2 (30 psi). Fig. 3(b) presents the stability test data measured by applying 0.4 V at an ambient pressure. The optimized carbon composite catalyst ("procedure – C") showed the current density of 2.0 A cm^{-2} at 0.2 V, and exhibited a steady-state current profile after 15 h.

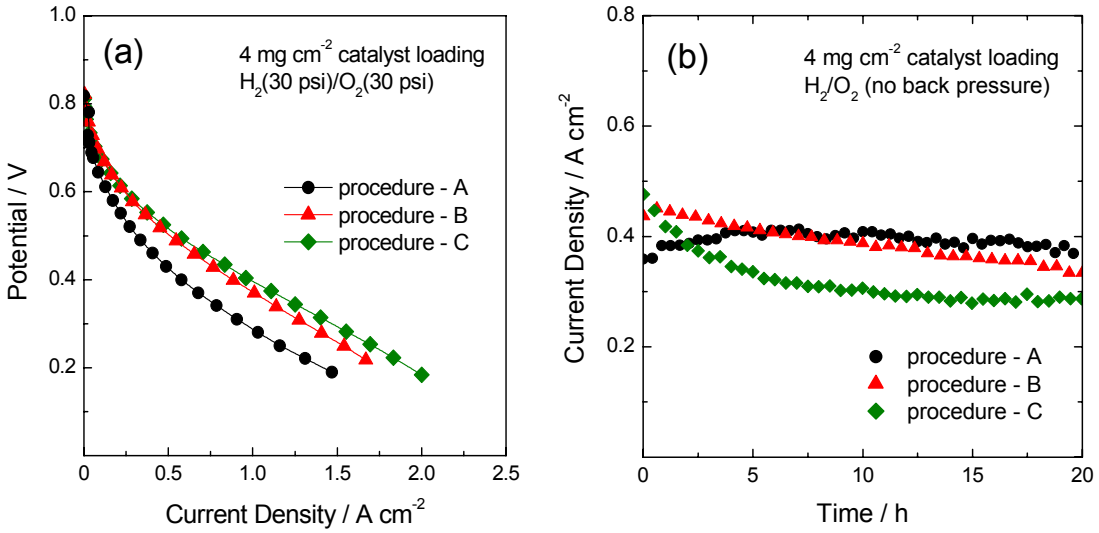

Figure 3. (a) Fuel cell performances and (b) stability test data (at 0.4 V) of the carbon composite catalysts prepared under different pyrolysis conditions.

Figure 4 shows the current density (stability test performance) measured on the carbon composite catalyst as a function of time. The cathode catalyst loading was 2 mg cm^{-2}, and the tests were run using H_2 (50 psi) and O_2 (50 psi). As indicated in the figure, the cathode compartment was periodically purged with O_2 gas during test, in order to remove liquid water accumulated inside the MEA. The result shows an initial increase of current density to ca. 0.6 A cm^{-2}, followed by a slight decay with time. The fuel cell performance was fully recovered upon O_2 purging, which indicates that an ineffective water management is responsible for a slight performance loss of fuel cell, and no irreversible loss of catalytic activity occurs.

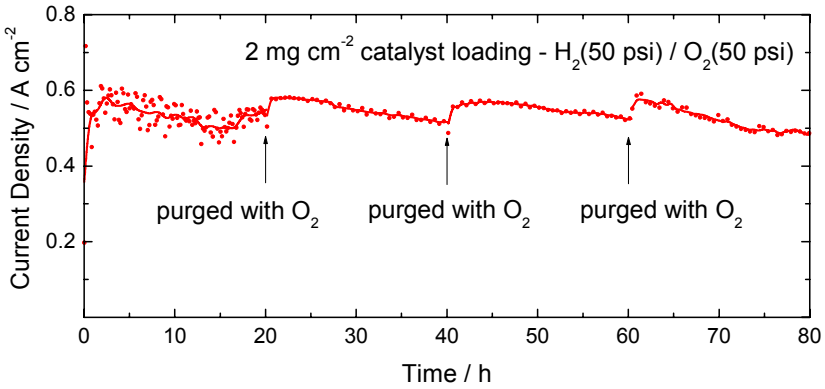

Figure 4. Typical stability test data (at 0.4 V) for the carbon composite catalyst.

Best performing catalysts are being tested under a variety of conditions – including (i) gas flow rate, (ii) back pressure, (iii) cell temperature, (iv) humidification temperature, and (v) gas diffusion layer, and advances in water management are being made. As an example, Figure 5 presents the stability test data obtained at 0.5 V for the carbon composite catalyst. The test was run at an ambient pressure for the cathode catalyst loading of 4 mg cm^{-2}. Note that no performance degradation was observed for 80 h of continuous operation without O_2 purging step.

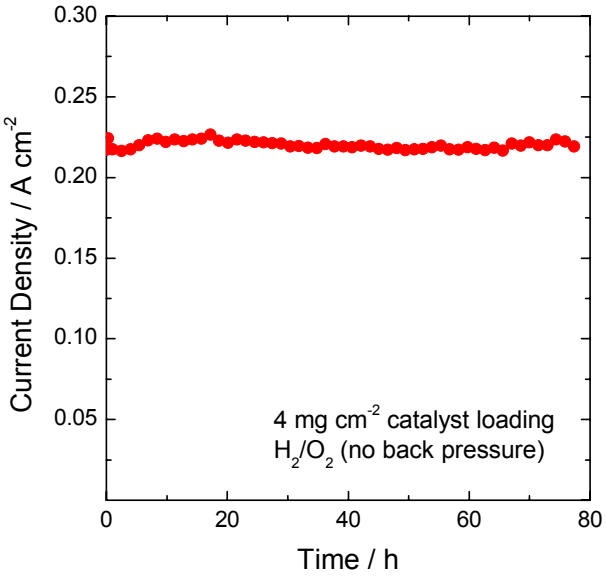

Figure 5. Stability test data of PEM fuel cell with the carbon composite catalyst performed without intermittent O_2 purging steps.

Conclusions

Carbon-based metal-free catalysts were synthesized by modifying the surface functional groups on the porous carbon black with low-cost organic precursors. Further, carbon composite catalysts were developed using a metal-free catalyst as a support through catalyzed pyrolysis followed by chemical post-treatments. Materials characterization studies indicated that the nature of nitrogen functional groups on the carbon surface and the carbon nanostructures play a critical role in the activity and stability of carbon-based catalyst. The catalytic activities as high as 1.3 A cm^{-2} (6 mg cm^{-2} loading) and 2.0 A cm^{-2} (4 mg cm^{-2} loading) at 0.2 V were obtained for the metal-free and carbon composite catalysts, respectively, in the fuel cell, and no irreversible activity loss was observed.

Acknowledgments

Financial support provided by the Department of Energy (contract no. DE-FC36-03GO13108) is acknowledged gratefully.

References

1. R. Jasinski, *Nature*, **201**, 1212 (1964).

2. A. Widelov, and R. Larsson, *Electrochim. Acta*, **37**, 187 (1992).
3. G. Lalande, R. Cote, D. Guay, J.P. Dodelet, L.T. Weng, and P. Bertrand, *Electrochim. Acta*, **42**, 1379 (1997).
4. R. Cote, G. Lalande, D. Guay, and J.P. Dodelet, *J. Electrochem. Soc.*, **145**, 2411 (1998).
5. P. Gouerec, M. Savy, and J. Riga, *Electrochim. Acta*, **43**, 743 (1998).
6. P. Gouerec, and M. Savy, *Electrochim. Acta*, **44**, 2653 (1999).
7. S. Lj. Gojkovic, S. Gupta, and R.F. Savinell, *Electrochim. Acta*, **45**, 889 (1999).
8. S. Lj. Gojkovic, S. Gupta, and R.F. Savinell, *J. Electroanal. Chem.*, **462**, 63 (1999).
9. M. Lefevre, J.P. Dodelet, and P. Bertrand, *J. Phys. Chem. B*, **104**, 11238 (2000).
10. H. Schulenburg, S. Stankov, V. Schunemann, J. Radnik, I. Dorbandt, S. Fiechter, P. Bogdanoff, and H. Tributsch, *J. Phys. Chem. B*, **107**, 9034 (2003).
11. S. Marcotte, D. Villers, N. Guillet, L. Roue, and J.P. Dodelet, *Electrochim. Acta*, **50**, 179 (2004).
12. K. Sawai, and N. Suzuki, *J. Electrochem. Soc.*, **151**, A682 (2004).
13. D. Villers, X. Jacques-Bedard, and J.P. Dodelet, *J. Electrochem. Soc.*, **151**, A1507 (2004).
14. K. Sawai, and N. Suzuki, *J. Electrochem. Soc.*, **151**, A2132 (2004).
15. S.-I. Yamazaki, Y. Yamada, T. Ioroi, N. Fujiwara, Z. Siroma, K. Yasuda, and Y. Miyazaki, *J. Electroanal. Chem.*, **576**, 253 (2005).
16. M. Yuasa, A. Yamaguchi, H. Itsuki, K. Tanaka, M. Yamamoto, and K. Oyaizu, *Chem. Mater.*, **17**, 4278 (2005).
17. F. Jaouen, F. Charreteur, and J.P. Dodelet, *J. Electrochem. Soc.*, **153**, A689 (2006).
18. R. Bashyam, and P. Zelenay, *Nature*, **443**, 63 (2006).
19. R. Yang, and A. Bonakdarpour, *ECS Trans.*, **3**, 221 (2006).
20. E.B. Easton, A. Bonakdarpour, R. Yang, D.A. Stevens, D.G. O'Neill, G. Vernstrom, D.P. O'Brien, A.K. Schmoeckel, T.E. Wood, R.T. Atanasoski, and J.R. Dahn, *ECS Trans.*, **3**, 241 (2006).
21. J.-H. Kim, A. Ishihara, S. Mitsushima, N. Kamiya, and K-I. Ota, *ECS Trans.*, **3**, 255 (2006).
22. T. Otsubo, S. Takase, and Y. Shimizu, *ECS Trans.*, **3** (2006).
23. N.P. Subramanian, S.P. Kumaraguru, H. Colón-Mercado, H. Kim, B.N. Popov, T. Black, and D.A. Chen, *J. Power Sources*, **157**, 56 (2006).
24. L. Liu, J.-W. Lee, and B.N. Popov, *J. Power Sources*, **162**, 1099 (2006).
25. L. Liu, H. Kim, J.-W. Lee, and B.N. Popov, *J. Electrochem. Soc.*, **154**, A123 (2007).